

Compton-profile anisotropies in graphite and hexagonal boron nitride

R. Tyk, J. Felsteiner, and I. Gertner

Department of Physics, Technion-Israel Institute of Technology, Haifa 32000, Israel

R. Moreh

Nuclear Research Center-Negev, Beer-Sheva, Israel and Ben-Gurion University of the Negev, Beer-Sheva, Israel

(Received 25 September 1984)

The Compton profiles of pyrolytic graphite and pyrolytic boron nitride have been measured in the directions of the c axis (J_{\parallel}) and perpendicular to it (J_{\perp}), using 60-keV γ rays of ^{241}Am . The anisotropy measured in boron nitride is found to be significantly smaller than that in graphite near zero momentum. This is consistent with the different character of the π electrons in the two materials. We find $J_{\parallel} - J_{\perp}$ to be negative near zero momentum for both graphite and boron nitride, the same as in all previously known measurements of graphite. To our knowledge, no other Compton anisotropy measurements of hexagonal boron nitride have been reported. Our results disagree with recently published linear combination of atomic orbitals self-consistent-field calculations, where $J_{\parallel} - J_{\perp}$ was found to be positive near zero momentum for both materials.

The isoelectronic compounds, graphite and hexagonal boron nitride (h -BN), have similar layered structures. However, their electronic properties are quite different due to the different character of their π electrons. Directional Compton profiles (DCP) of graphite have already been measured and calculated by a number of groups¹⁻⁵ in order to investigate the anisotropy in the electron momentum distribution. In addition to graphite, Dovesi, Pisani, Roetti, and Dellarole³ have also calculated the DCP of h -BN; however, no DCP measurements of h -BN have been reported.

In all previous measurements of graphite, the DCP parallel to the c axis (J_{\parallel}) were found to be smaller than the DCP perpendicular to the c axis (J_{\perp}) near zero momentum. Both the pseudopotential calculation and the molecular-orbital calculation of Reed, Eisenberger, Pandey, and Snyder¹ on graphite show this same feature. Dovesi *et al.*³ have calculated the DCP in both graphite and h -BN, using the linear combination of atomic orbitals (LCAO) self-consistent-field method, obtaining $J_{\perp} < J_{\parallel}$ near zero momentum in both materials. Their result for graphite, which is the most recent, contradicts all previous measurements and calculations. In the present work, we have remeasured the DCP of graphite as well as measured for the first time the DCP of h -BN. It will be shown that our results for both graphite and h -BN also contradict the calculations of Dovesi *et al.*³

The Compton profile is derived from the energy spectrum of γ rays inelastically scattered from the sample to be investigated. A general review on Compton-profile measurements has been given in Ref. 6. In the present work, we used 59.54-keV γ rays from a 5-Ci ^{241}Am annular source. The scattering angle was 169.5° . The scattered γ rays were measured with an intrinsic Ge detector. The resolution of the spectrometer was 365 eV [full width at half maximum (FWHM)] at 60 keV. This means a resolution of 0.53 a.u. of momentum near the peak of the profile.

Since large crystals of graphite and h -BN are not available, we used pyrolytic graphite and pyrolytic h -BN to measure the anisotropy of the momentum distribution. Thus,

we only measured the distribution parallel to the c axis (J_{\parallel}) and the average distribution normal to the c axis (J_{\perp}). Both graphite and h -BN samples consisted of two pieces of $0.65 \times 0.65 \times 2.52$ cm³ each, with the c axis normal to the longest dimension. By turning the pieces by 90° , it was possible to measure J_{\parallel} and J_{\perp} with identical geometry. Both samples of graphite and h -BN were supplied by Union Carbide. The mosaic spread of both samples was measured by using x-ray diffraction, and was found to have a FWHM of $53 \pm 1^\circ$ for graphite and $106 \pm 2^\circ$ for h -BN. In the case of graphite, a confirmation of the mosaic spread value was obtained using neutron diffraction, while that of h -BN was confirmed using a new nuclear method.⁷ Despite these large values, a clear difference between J_{\parallel} and J_{\perp} was observed. If the distribution of the c axes of the crystallites in the samples is taken to be Gaussian, one has $F(\theta) \propto \exp(-\theta^2/\sigma^2)$. Then, in order to compare with experiment, one has to smear the theoretical profiles by averaging over all c axes directions with the weight $F(\theta)$. The theoretical profile at any particular direction was derived from an expansion in Y_{00} and Y_{20} . It turned out that 53° mosaic spread reduces the maxima and minima of the anisotropy by 25%, while 106° mosaic spread reduces the anisotropy by 65%. A similar smearing should further be made on the theoretical profiles to account for the fact that the γ -ray source was annular.⁸ This increases the former smearing to 31% for 53° mosaic spread and 69% for 106° mosaic spread. In spite of this reduction, it is still possible to check the agreement between the experimental data and the various theoretical predictions.

The data were collected in 2048 channels. The separation between channels corresponded to an interval of approximately 0.06 a.u. About 300 000 counts were accumulated at the channel of the Compton peak for each sample, during a period of less than half a day. The data analysis included background subtraction, absorption correction, and a Monte Carlo correction for multiple scattering.⁹ Fourier deconvolution and filtering was done so that the data still contain a smearing with Gaussian resolution function of

0.53 a.u. FWHM.

The measured DCP of graphite and *h*-BN are given in Table I. In Fig. 1, we compare our measured Compton-profile anisotropy $J_{\parallel} - J_{\perp}$ in graphite with the previous measurements of Reed *et al.*,¹ Paakkari,² and Loupias, Chomilier, and Guérard.⁴ Although each measurement had different resolution and different sample quality, the essential features in the anisotropy curves appear to be the same in all of them. In Fig. 2, our anisotropy measurement in graphite is compared with the pseudopotential calculation and the molecular-orbital calculation of Reed *et al.*,¹ and with the LCAO calculation of Dovesi *et al.*³ The theoretical curves are shown after the corresponding Compton profiles have been convolved with the Gaussian resolution function, and also smeared for the effects of the mosaic spread and the annular source geometry. The two calculations of Reed *et al.*¹ produce the same oscillations as experiment, but with larger amplitudes. On the other hand, the calculation of Dovesi *et al.*³ shows different features below 1 a.u. In particular, it produces positive values of $J_{\parallel} - J_{\perp}$ near zero momentum.

In Fig. 3, we show our measured anisotropy for *h*-BN, together with the corresponding calculation of Dovesi *et al.*³ Since the smearing effect of the mosaic spread is rather large in our *h*-BN experiment, we show the theoretical curve of Dovesi *et al.*,³ once smeared with the effects of the mosaic spread and the annular source geometry, and once without those effects. This calculated *h*-BN anisotropy has

TABLE I. Experimental Compton profiles of graphite and *h*-BN.

q (a.u.)	Graphite		<i>h</i> -BN	
	J_{\parallel}	J_{\perp}	J_{\parallel}	J_{\perp}
0.0	2.087	2.121 ± 0.005	4.170	4.173 ± 0.008
0.1	2.078	2.109	4.149	4.150
0.2	2.050	2.071	4.086	4.085
0.3	2.002	2.013	3.981	3.977
0.4	1.933	1.937	3.841	3.831
0.5	1.843	1.846	3.667	3.651
0.6	1.732	1.732	3.450	3.435
0.7	1.603	1.603	3.196	3.191
0.8	1.459	1.464	2.916	2.926
0.9	1.309	1.323	2.624	2.649
1.0	1.158	1.181	2.333	2.370
1.1	1.013	1.040	2.055	2.096
1.2	0.881	0.907	1.798	1.836
1.3	0.767	0.786	1.569	1.599
1.4	0.671	0.677	1.370	1.387
1.5	0.590	0.582	1.201	1.208
1.6	0.521	0.504	1.060	1.056
1.7	0.463	0.440	0.944	0.928
1.8	0.417	0.391	0.848	0.825
1.9	0.379	0.352	0.768	0.745
2.0	0.346	0.321 ± 0.002	0.699	0.681 ± 0.004
2.2	0.293	0.276	0.593	0.582
2.4	0.257	0.244	0.521	0.510
2.6	0.227	0.219	0.458	0.450
2.8	0.201	0.199	0.407	0.401
3.0	0.181	0.181	0.363	0.363
3.5	0.141	0.143	0.281	0.283
4.0	0.111	0.113	0.221	0.223
4.5	0.088	0.088	0.176	0.176
5.0	0.070	0.070	0.141	0.139

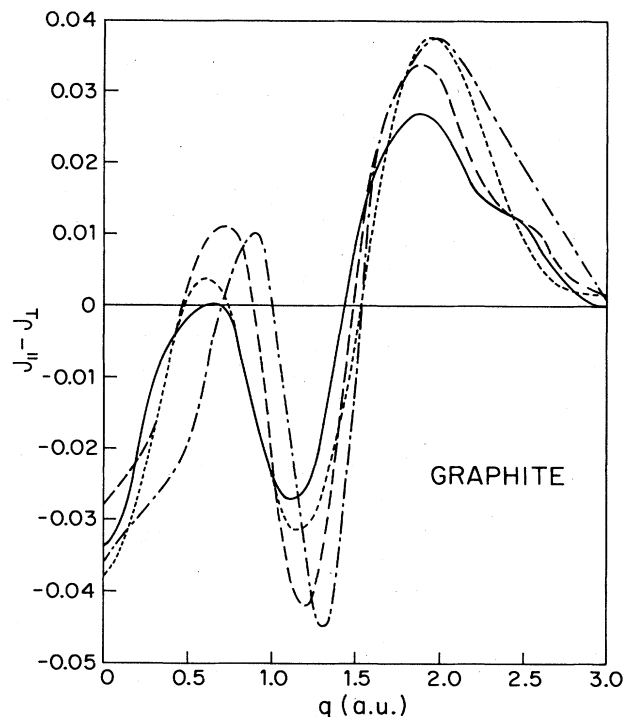


FIG. 1. Compton-profile anisotropy of graphite. Solid line is the present measurement. Short-dashed curve is the measurement from Ref. 2. Long-dashed curve is the Ref. 1 measurement. Chained curve is the Ref. 4 measurement.

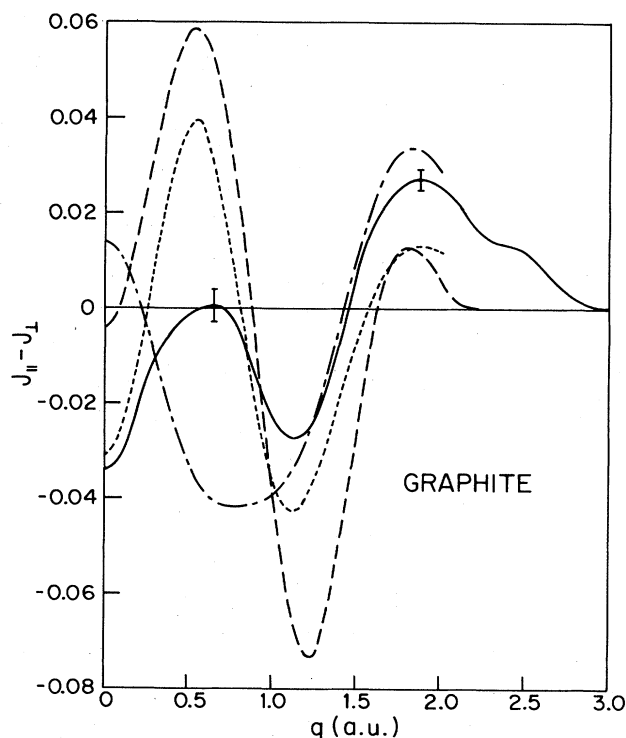


FIG. 2. Compton-profile anisotropy of graphite. Solid line is the present measurement. Short-dashed curve is the molecular orbital calculation from Ref. 1. Long-dashed curve is the pseudopotential calculation from Ref. 1. Chained curve is the LCAO calculation from Ref. 3. The theoretical curves have been smeared for the effects of experimental resolution, mosaic spread, and annular source geometry.

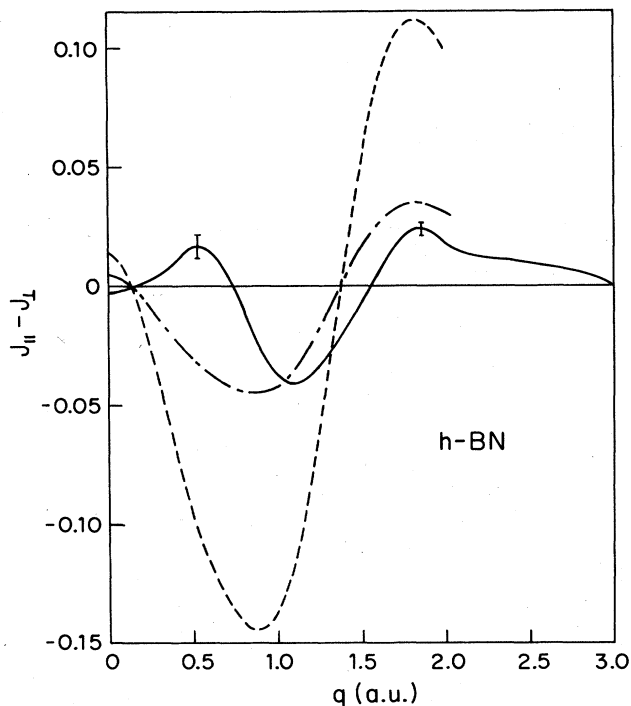


FIG. 3. Compton-profile anisotropy of *h*-BN. Solid line is the present measurement. Dashed curve is the LCAO calculation from Ref. 3, smeared only for the effect of experimental resolution. Chained curve is the same calculation smeared also for the effects of mosaic spread and annular source geometry.

the same features as that calculated for graphite by the same authors and disagrees with our experiment, especially at low momenta.

Finally, we compare in Fig. 4 our measured Compton-profile anisotropies for graphite and *h*-BN. Taking into ac-

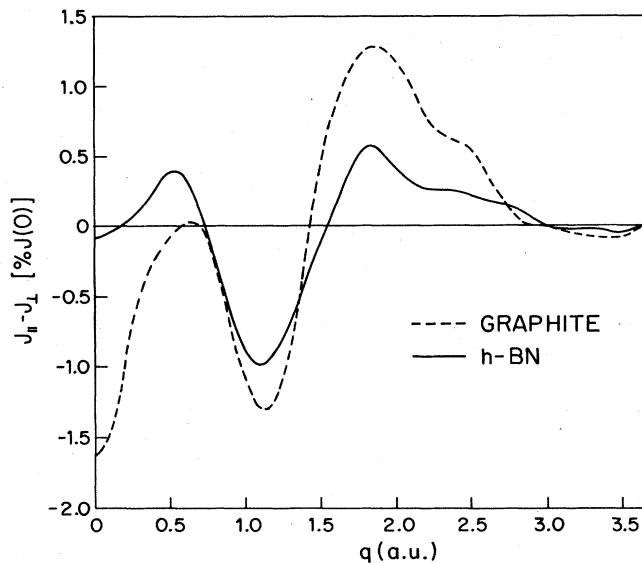


FIG. 4. Comparison of the present measurements of the Compton-profile anisotropy of graphite and *h*-BN.

count the smearing effect of the mosaic spread in *h*-BN, the anisotropies of the two materials above 0.8 a.u. are remarkably similar. This is largely due to the similar crystal structures of graphite and *h*-BN. On the other hand, the low-momentum part of the anisotropy is different in the two materials, since the low-momentum region is governed by the behavior of the outer electrons. In particular, the itinerant nature of the π electrons in the basal planes in graphite, which is not the case in *h*-BN, should explain why the Compton-profile anisotropy in graphite is much more negative than the anisotropy in *h*-BN, at low momenta.

¹W. A. Reed, P. Eisenberger, K. C. Pandey, and L. C. Snyder, *Phys. Rev. B* **10**, 1507 (1974).

²T. Paakkari, *Phys. Fenn.* **9**, 185 (1974).

³R. Dovesi, C. Pisani, C. Roetti, and P. Dellarole, *Phys. Rev. B* **24**, 4170 (1981).

⁴G. Loupiaz, J. Chomilier, and D. Guérard, *J. Phys. (Paris) Lett.* **45**, L301 (1984).

⁵S. Vasudevan, T. Rayment, B. G. Williams, and R. Holt, *Proc. R. Soc. London, Ser. A* **391**, 109 (1984).

⁶*Compton Scattering*, edited by B. G. Williams (McGraw-Hill, London, 1977).

⁷R. Moreh, W. C. Sellyey, and R. Vodhanel, *Phys. Lett.* **92B**, 286 (1980).

⁸O. Aikala, *Phys. Status Solidi B* **110**, K107 (1982).

⁹J. Felsteiner, P. Pattison, and M. Cooper, *Philos. Mag.* **30**, 537 (1974); J. Felsteiner and P. Pattison, *Phys. Rev. B* **13**, 2702 (1976).